Original Research Article

SYNTHESIS AND CHARACTERIZATION OF CRAB SHELL BASED MAGNETIC NANOPARTICLES FOR THE REMEDIATION OF ABATTOIR WASTE WATERS

Abstract; Meat and beef consumption rate in Nigeria has recorded increment leading to increase in abattoirs and lack of control in discarding the waste of the slaughtered animals has heightened the rate of ground water, air and environmental pollutions. In this paper, crab shell based magnetic nano particles was utilized in the purification of waste water from abattoir. The factors considered in the purification process were pH, dosage, initial concentration, temperature and time and the response includes: BOD, COD Turbidity and color. Prior to the experimentation in the laboratory, the central composite design (CCD) of the experimental design was carried to determine the number of levels and the possible number of experimental runs during laboratory experiment. The outcome of the laboratory was used for the response surface methodology (RSM) of which linear and interaction model ware utilized in the determination of the relation between the factors and the responses and the model type was multiple input single output model system (all the factors equated to one response per time). Analysis of variance (ANOVA) tables was utilized in the determination of the model performance for each response to determine the best model suitable for the prediction of the responses. From the results obtained, the R-square values from the ANOVA table showed that the interaction model had a better prediction accuracy of 65.75%, 33.65%, 60.73% and 59.74% for the prediction of BOD, COD, turbidity and colour responses respectively. The interaction model being the best was deployed for the generation of surface and contour plots to graphically obtain the optimal responses and factors that was utilized as a first guess to the optimization of the model and the final optimal response values obtained were 4.33mg/l, 128.9mg/l, 39.87% and 33.41% for BOD, COD, turbidity and colour respectively at the optimal factor conditions of 5.5, 0.68g, 260mg/l 335k and 50mins for pH, dosage, initial concentration, temperature and time respectively.

Keywords; *waste water treatment, Abbattoir, Nano-particles, responses, factors, modeling and optimization*

1. Introduction;

Nanoparticles was defined by [1,3] as the characteristics of solid distribution having a size range of 10-1000nm. Most of the nano-particles utilized are designed from many materials and components and such nano-particles are known as nano-composites. Nano-particles are usually synthesized from different sources mainly from natural and synthetic sources [2,4]. In this regard, the use of crab shell has been known to exhibit high efficient characteristics for utilization in the water purification processes which its properties are due to biosorbent of its shell as the result of its high mechanical strength, strong structure and its capacity of withstanding extreme conditions during the nano-particles synthesis

process [3,5]. [4,6,7] made contributions in improving the waste water purification properties of the waste water which includes infusion of iron oxide into the internal structure with the aim of upgrading the magnetic properties of the nano-particle.

There policies on waste water management and pollution in Nigeria but the inability to enforce the policies has been major cause of lack of disposal control as the abattoir waste are disposed to the environment and to the water bodies resulting to the death of aquatic animals. Some of the animal process are performed close to a river causing nuisance to the aquatic bodies [8]. The waste water from abattoirs comprises of effluents from the slaughter house and with high amount of suspended solids, liquids and fats from the animals [9]. In Nigeria, there has been a high demand for meat, leading to the drive to maximize the meat production which has led to failure in adhering the good manufacturing practices during the meat processing and resulting to a total neglect of good hygiene practice and safety process [9, 10]. The processing of meats from cows and other mammals requires large amount of water leading to the generation of large amount of suspended solids which affects both the surface water and the underground water because the processing of slaughtered animals generates urine, fats, blood and manure that are washed with water and sent to river bodies [11]. Hence, this paper presents the use of chito-protein nano-particles obtained from crushed exoskeleton of crab shell for the purification of the waste water from slaughter houses. Characterization was carried out on the raw shell of the craw to determine the physicochemical properties. The nano-particles prepared was usedin the adsorption process of the waste water to determine the quantity of the responses. As guide to the laboratory experiment, CCD of experimental design was done with design expert to determine the amount of responses removed from the waste water. The responses were COD, BOD, turbidity and colour. The factors considered were pH, dosage, initial concentration, temperature and time. Linear and interactive RSM models were utilized in the development of relationship between the factors and the responses and ANOVA table was deployed for the determination of the performance of the models deployed to obtain the best model based on the prediction performance and genetic algorithm (GA) was utilized for the determination of the optimal responses and factors. The modeling was carried out in MatLab 2015a. the outcome of this paper would suggest means of purifying waste water from slaughter house was crab shell nano-particles as the adsorbent.

2. Literature Review

In [12]. coagulation/flocculation process was used at laboratory bench scale for the removal of chemical oxygen demand (COD), total suspended solids (TSS) and total phosphorus (TP) in abattoir wastewater. The wastewater was allowed to settle for 24 h and TSS and TP removal efficiencies of 65% and 32% were achieved, respectively. They used alum, ferric chloride and ferric sulfate during the coagulation/flocculation process. From their results, they observed that alum proved more effective in the reduction of TSS and TP present in the wastewater, whereas ferric sulfate was more effective in the reduction of COD. Increasing the dose of alum to 750 mg/l caused the removal efficiency of TP to reach 45%. According to the authors, the rate of removal of TP linearly increased with increasing doses of alum, resulting in a 98% removal efficiency of TP at 1000 mg/l

dose of alum. At a 95% confidence interval, alum dose, coagulation velocity gradient/rapid mixing time (coagulation Gt) and flocculation velocity gradient/slow mixing time (flocculation Gt) were not significant for TSS removal efficiency, but alum dose was significant for TP removal. They also observed that the addition of a polyelectrolyte to an inorganic coagulant proved effective in the reduction of COD, TSS and TP, cut the amount of coagulant used and reduced the cost of the coagulation/flocculation process. A significant degree of particle elimination by size was produced by using alum; this improved further with the addition the polyelectrolyte.

In [13,14], the author studied the slaughterhouse waste water treatment using combined chemical coagulation and electrocoagulation process. The authors employed the use of poly aluminium chloride (PACl) and applied voltage to the treatment of slaughter house waste water. An efficiency of more than 99% removal in the levels of BOD5 and COD was achieved by using a coagulant dose of 100mg/L and an applied voltage of 40V. Chemical coagulation of slaughterhouse wastewater has also been studied by adding aluminum salts and polymer compounds, and a maximum COD removal efficiency of 45–75% has been reported in[16,17]. Polyaluminum chloride (PACl) is commonly used as the flocculant to coagulate small particles into larger flocs that can be efficiently removed in the subsequent separation process of sedimentation and/or filtration. [18], studied the treatment of slaughterhouse wastewater characterized as having exceptionally high BOD, COD and TSS contents. The authors used a combined treatment system of coagulation and adsorption onto activated carbon, using different coagulants, such as alum, lime, ferrous sulfate, and ferric chloride were individually and in combination. A jar test method was applied to determine the optimal dose of these coagulants. From the results, they observed that increasing dosages of coagulants increased the sludge formation and COD removal. They observed that the volume of sludge was found to be an indicator of maximum removal of COD. From their studies, alum coagulant proved to be the best in removing COD up to 92%. Maximum sludge volume (400 ml/L) was also observed with alum. More than 90% removal efficiency in pollution load was observed at the set optimal conditions with coagulation process. A combination of coagulation and adsorption processes made negligible improvement in the removal efficiency of the system (as compared to the single process of coagulation) and removed pollution load up to 96%. [19] discovered that with inorganic flocculants, the effective species can be a solvated metal ion, which affect flocculation through double-layer compression and Schulze-Hardy effects and with an increase in pH, these species become charged and the mechanism of action changes. When the colloids are hydrophilic, e.g. humic acids, pH affects protonation. In presence of ionisable acidic or basic groups, colloid surface charge is affected by pH changes. In organic polymer flocculation as well, pH can affect polymer activity and the mechanism. From the research carried out in [20,21], it shows that pH of water adjusted with sulfuric acid and alum ranging from 5.0-8.0 gave an optimum pH of 7.0, and this gave the best color removal at about 76% and the turbidity removal around 80%. Research in [22] shows that the optimum value of pH depends essentially on the properties of the water treated, type of the coagulant used and its concentration. The results he obtained showed that the optimum initial pH for turbidity removal is 7 and 8.6 giving removal efficiencies of 95.9% and 95.2%, respectively. In a research conducted in [23], higher concentration of effluent gives rise to decreased degree of flocculation, and the particles may be completely covered by the

absorbed polymer layer. Higher concentration of effluent means higher amount of suspended particles and larger quantity of biodegradable materials contained in the water.

3. Methods

3.1 Collection of samples and Pre-processing

The waste water utilized in this study was obtained from the local abattoir located in Amansea in Awka south Local government area (LGA) Anambra State state in south eastern Nigeria.the waste water sample was sieved to remove large suspended solids and other solids waste and the filtered sample was stored in a refrigerator. The crabshell was acquired from Onitsha Main market the Anambra state, The shells were washed, sundried and crushed to particle sizeof 75 microns.

3.2 Characterization of Waste water sample

The method utilized for the determination of COD in the waste water was from [24]. 10 ml of 0.25 N of potassium dichromate (k2Cr2O7) and 30 mlof sulphuric acid + silver nitrate reagent was prepared in 20 ml dilute sample. Themixture was re-fluxed for 2 hours and allowed to cool to a temperature of 28C. Distilled water will be used to dilute the solution making a volume of 150 ml. the remaining amount of potassium dichromate was titrated with ferrous ammonium sulphate (FAS) using ferion indicator, the COD for each solution was obtained based on equation 1 below [24].

$$COD = \frac{(F_b - F_s) \times n \times 1000 \times 8}{V_s} \qquad (1)$$

Where F_b represents amount of FAS in blank (ml), F_s represents the amount of FAS in the sample (ml), n represents the normality of FAS, the value 8 was taken as the equivalent weigth of oxygen [25] and V_s represents the volume of the sample.

Turbidity meter and pH meter were used to determine the turbidity and pH of the waste water.

UV visible spectrophotometer was utilized at wavelength of 420nm to determine the colour of the sample.

3.3 Magnetic Composite synthesis

Synthesis of the crabshell based magnetic nano-particle was done in two stages as detailed in [20, 22, 24, 25]. chito-protein was extracted from waste crabshell through de-protenization procedure with the utilization of sodium hydroxide. 500 ml of 2M NaOH solution was contacted with 100 g of crab shell using a magnetic hotplate stirring at 200 rpm and 65C for 2 h. After cooling, the mixture was allowed to settle and then filtered. The filtrate was subjected to centrifugation and a clear liquid product was decanted to give way for highly concentrated radical protein sludge. The sludge product was dried at 1500C for 6 h. The obtained chito-protein product was stored in a dry container for further utilization.

Ferromagnetite was synthesized via co-precipitation method with a molar ratio of 1:2 for Fe (II):Fe (III), respectively. The mixture was dissolved in de-ionized water and stirred at

50 rpm for 3 h (Sibiya et al., 2022; Kristianto et al., 2020). Subsequently, dried crabshell chito-protein was added to the solution in a ratio of 1:1. the mixture will be homogenized for 1 h, followed by decantation. The formed precipitate was dried in an oven at 80C for 80 min. The resulting product will be labeled MCSNP which will be used to facilitate the remediation of abattoir wastewater.

3.4 Design of Experiment

Based on literature survey, the table for range of values of the factors for abattoir waste water treatment with MCNSC was shown in Table 1.

Table 1; Range of values for the factors

Factors	Range
pH	4-8
Dosage(g)	0.5-1.1
Init conc(mg/L)	100.5-400.5
Temp (K)	310-345
Time (mins)	15-50

The range values of the factors was entered in the design software application to generate the factor levels which was generated and shown in table 2.

Table 2; factor levels

Factors	-alpha	-1	0	1	alpha
pH	3	4	6	8	9
Dosage(g)	0.35	0.5	0.8	1.1	1.25
Init conc(mg/L)	25.5	100.5	250.5	400.5	475.5
Temp (K)	301.25	310	327.5	345	353.75
Time (mins)	6.25	15	32.5	50	58.75

The outcome from the factor levels was used to generate the experimental runs that was taken to the laboratory for the purification of the waste water.

3.5 Laboratory Experiment for the waste water purification

Five different concentrations of effluent was prepared prior to each batch adsorptive-coagulation experiment and the initial conditions of temperature, turbidity and absorbance was recorded. The pH of the samples was adjusted to desirable values using very few drops of 0.5 M sulphuric acid and (or) 0.5 M sodium hydroxide solutions. Different amounts of MCSNC was added and the five beakers was stirred simultaneously at 250 rpm for 3 min to initiate the coagulation process while the flocculation process was carried out by slow stirring at 20 rpm for 30 minutes, as described in [26,27]. After the slow stirring, the mixtures was allowed to settle by gravity, samples was withdrawn from the beaker and tested for the turbidity and color removal at different withdrawal time.

3.12 RSM modeling and Optimization

To determine the best parameters for optimum pigment and turbidity removal, genetic algorithm (GA) optimization techniques will be adopted. genetic algorithm (GA) entails, a statistical exploration technique, capable of simulating a natural biological evolution is usually implemented in solving the optimization problems. The developed RSM model will be coupled with GA and used as a decision parameter in GA optimization (which occurs through a 4-staged cycle). The best sequence produced at the convergence of the loop becomes the solution to the optimization problem [28, 29] GA optimization will be carried using the optimization toolbox of MATLAB R 2015 b (Matworks Inc.). The RSM models utilized were linear model and interaction models as shown in equations 2 and 3 respectively.

$$Y = a_o + a_1x_1 + a_2x_2 + a_3x_3 + a_4x_4 + a_5x_5 \quad (2)$$

$$Y = a_o + a_1x_1 + a_2x_2 + a_3x_3 + a_4x_4 + a_5x_5 + a_6x_1x_2 + a_7x_1x_3 + a_8x_1x_4 + a_9x_1x_5 + a_{10}x_2x_3 + a_{11}x_2x_4 + a_{12}x_2x_5 + a_{13}x_3x_4 + a_{14}x_3x_5 + a_{15}x_4x_5 \quad (3)$$

Where Y represents the responses (color, turbidity, COD and BOD) which implies that there was four models for each RSM models which represents each of the responses, x_1 to x_5 are the factors namely: pH, dosage, initial concentration, temp and time respectively.

4. Results

4.1 Characterization

The waste water physiochemical characterization outcome was shown in table 3.

Table 3; physiochemical characterization

Parameters	Raw waste water effluent	Treated waste water effluent
Turbidity (mg/L)	595	63
Total suspended solids (mg/L)	1030.8	2.5
Total solids (mg/L)	1614.8	2.1
Biological oxygen demand (mg/L)5	220	8.6
Chemical oxygen demand (mg/L)	692	152
COD/BOD5	3.145	17.67
pH	7.5	8.1
Total phosphorus, mg/L	77.6	4.3
Alkalinity as CaCO3 (mg/L)	1.4217	0.2294
Sulphate as SO4 (mg/L)	13.62	-
Iron (mg/L)	3.08	-
Sodium as Na (mg/L)	35.855	25.1072
Potassium as K (mg/L)	0.5096	0.3579
Oil and grease (mg/L)	1.546	1.1026
Odour	Offensive	Odourless
Colour	Dark red	colourless

The FTIR of the nano-particle was shown in figure 1.

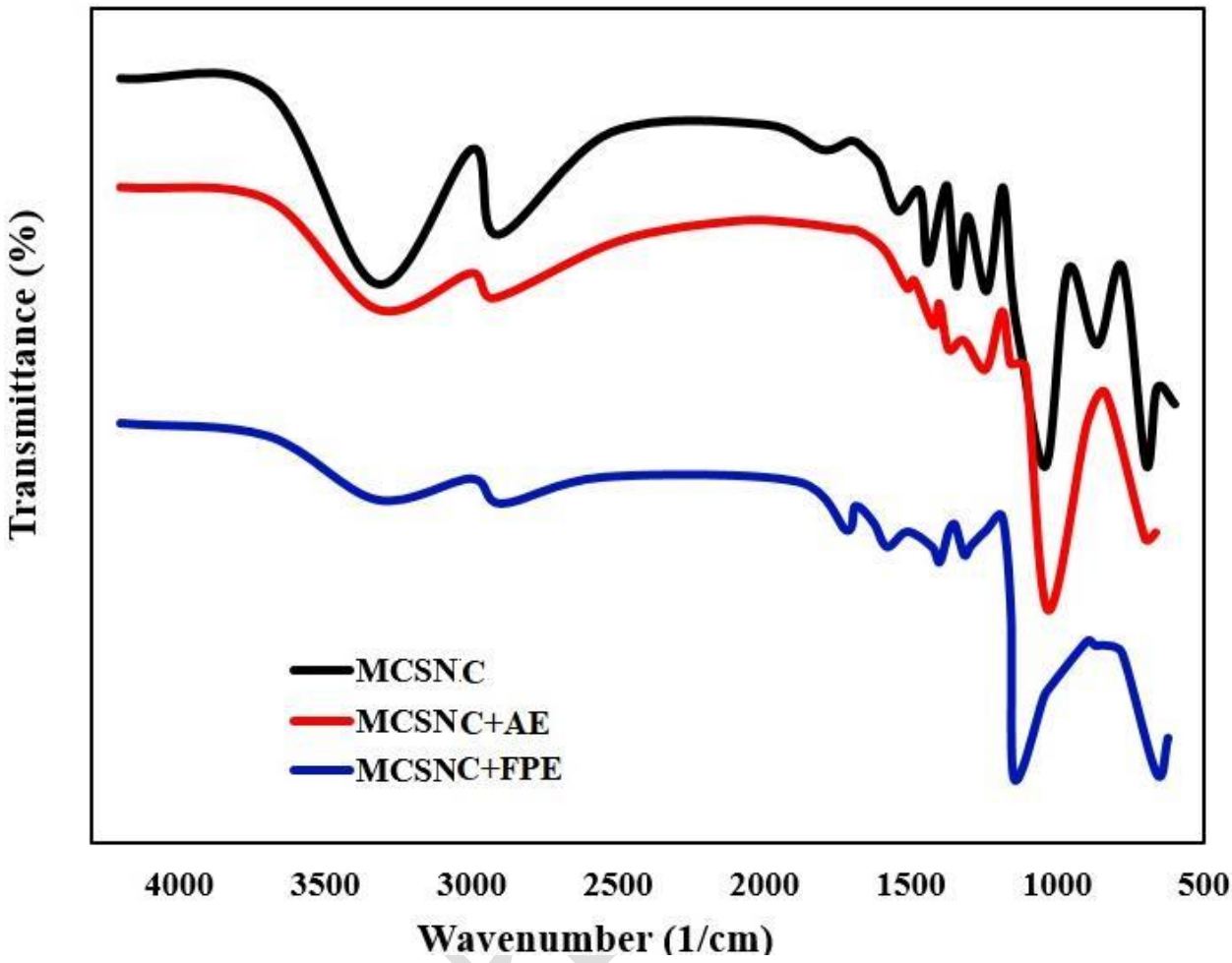

Figure 1; FTIR Spectra of pure and spent nano-particle (MCSNC)

The crab shells gave a yield of 34 ± 0.5% chito-protein. The FTIR spectra of MCSNC, MCSNC+AE and MCSNC+FPE are depicted in figure 1, the FTIR spectra of MCSNC vibrational peaks observed from the analysis were made at 3324.8, 2922.2, 1570, 1513.3, 1363.5, 1028, 898.3, and 662.4 cm^{-1}. Usually the absorption peaks observed below 500 cm-1 are not applicable for the characterization of crab shell (Kristianto et al., 2020; Ohale et al., 2020). The strong peaks at 1028 and 662.4 cm-1 may be attributed to Fe-O lattice bending vibration resulting from the fero-magnetic co-precipitation step of MCSNC synthesis. The absorption peak at 898.3 cm^{-1} indicates the existence of aliphatic C-N stretching group in the crab shell. The wave-number at 1363.5 cm^{-1} can be assigned to C-H bending of side chain –CH2OH and presence of β-esters. The absorption peak at 3324.8 cm^{-1} which is within the range of 3300 and 3500 cm^{-1} is characteristic of N-H of amides, (Coutts, 2008). Studies in literature about FTIR spectroscopy related with crabshell chito-protein showed that characteristic peaks at 2922 cm-1, 1513.3 cm^{-1} and 1570 cm-1 are After adsorptive-coagulation treatment of abattoir and fishpond effluents, FTIR results of spent MCSNC (MCSNC+AE and MCSNC+FPE) showed discernible vibrational deviations, and disappearance of some peaks. The N–H bending vibration of amide II band, observed at 1513.3 cm^{-1} in the original adsorbent, completely disappeared following abattoir effluent

treatment (MCSNC+AE). Similarly, C-N stretching vibration completely collapsed following treatment of both effluents. These significant reductions and disappearance of peaks illustrate the substantialcharacterized demonstrate the presence of –CH3, –CH2, N–H bending vibration of amide II band, and N–H bending vibration of primary amides (Choi *et al.*, 2007). participation of these functional groups in the treatment of abattoir and fishpond effluents.

4.2 Results of the experimental design, RSM, ANOVA and Optimization

The results of experimental design for abattoir waste water coagulation using MCSNC was shown in Table 4.

Table 4; experimental design with laboratory outcome

Run	pH	dosage	Initial conc (mg/L)	Temp (K)	Time (mins)	BOD (mg/L)	COD (mg/L)	Turbidity (%)	Color (%)
1	8	0.50	100.50	310.00	50.00	18.31	180.55	36.09	33.11
2	4	0.50	100.50	310.00	15.00	0.36	176.80	97.74	94.76
3	8	1.10	100.50	310.00	15.00	13.22	193.64	41.33	38.35
4	4	1.10	100.50	310.00	50.00	0.26	155.26	91.61	88.63
5	8	0.50	400.50	310.00	15.00	25.80	212.54	51.44	48.46
6	4	0.50	400.50	310.00	50.00	4.50	174.15	85.42	82.43
7	8	1.10	400.50	310.00	50.00	3.87	168.03	81.17	78.18
8	4	1.10	400.50	310.00	15.00	1.31	184.28	83.38	80.40
9	8	0.50	100.50	345.00	15.00	1.19	196.00	95.42	92.44
10	4	0.50	100.50	345.00	50.00	4.09	157.61	86.16	83.18
11	8	1.10	100.50	345.00	50.00	3.13	153.71	79.15	74.57
12	4	1.10	100.50	345.00	15.00	2.92	149.97	81.27	76.68
13	8	0.50	400.50	345.00	50.00	1.08	150.02	73.65	69.06
14	4	0.50	400.50	345.00	15.00	3.17	136.27	88.06	83.48
15	8	1.10	400.50	345.00	15.00	18.98	180.89	28.90	24.31
16	4	1.10	400.50	345.00	50.00	3.08	142.51	79.09	74.49
17	8	0.50	100.50	327.50	32.50	15.61	153.29	42.54	37.96
18	4	0.50	100.50	327.50	32.50	2.12	123.56	81.83	77.25
19	8	1.10	100.50	327.50	32.50	3.59	164.18	76.17	71.59
20	4	1.10	100.50	327.50	32.50	1.22	153.75	67.90	63.32
21	8	0.50	400.50	327.50	32.50	0.94	162.45	86.92	71.34
22	4	0.50	400.50	327.50	32.50	8.06	159.67	79.10	63.52
23	8	1.10	400.50	301.25	32.50	5.90	157.68	78.56	74.97
24	4	1.10	400.50	353.75	32.50	0.29	124.26	87.46	83.88
25	8	0.50	100.50	327.50	6.25	5.60	140.86	88.82	85.23
26	4	0.50	100.50	327.50	58.75	0.14	113.00	97.96	94.38
27	8	1.10	100.50	327.50	32.50	2.41	125.43	83.01	79.43
28	4	1.10	100.50	327.50	32.50	1.93	104.93	87.26	83.68
29	8	0.50	400.50	327.50	32.50	5.10	128.10	75.32	71.74
30	4	0.50	400.50	327.50	32.50	0.90	116.90	91.08	87.50
31	8	1.10	400.50	327.50	32.50	0.70	123.70	82.59	79.01
32	4	1.10	400.50	327.50	32.50	1.13	124.13	90.23	86.65

The ANOVA table for BOD linear and interaction models was shown in table 5 and table 6 respectively.

Table 5; ANOVA table for Linear model

Coefficient variable	Coefficient values	Sum of square (SE)	T-statistics	P-value	Statistical parameters
a_0	30.4760	25.1811	1.2103	0.2371	R^2 = 0.2989
a_1	1.2683	0.5212	2.4336	0.0221	adjR^2 = 0.1641
a_2	-3.4406	3.4264	-1.0042	0.3246	mse = 33.8112
a_3	0.0018	0.0069	0.2648	0.7933	rmse = 5.8147
a_4	-0.0858	0.0739	-1.1615	0.2560	

a_5	-0.0814	0.0739	-1.1018	0.2807	

Table 6; ANOVA table for Interaction model

Coefficient variable	Coefficient values	Sum of square (SE)	T-statistics	P-value	Statistical parameters
a_0	45.0690	110.9462	0.4062	0.6900	R^2 = 0.6575
a_1	22.9104	11.1817	2.0489	0.0572	adjR^2 = 0.3365
a_2	-159.9352	77.2337	-2.0708	0.0549	mse = 26.8385
a_3	-0.0034	0.1550	-0.0220	0.9827	rmse = 5.1806
a_4	-0.2170	0.3332	-0.6512	0.5241	
a_5	0.6301	1.4133	0.4458	0.6617	
a_6	-0.6824	1.5749	-0.4333	0.6706	
a_7	-0.0013	0.0031	-0.4155	0.6833	
a_8	-0.0586	0.0336	-1.7415	0.1008	
a_9	-0.0410	0.0336	-1.2190	0.2405	
a_{10}	-0.0042	0.0206	-0.2019	0.8425	
a_{11}	0.5158	0.2294	2.2484	0.0390	
a_{12}	-0.2299	0.2294	-1.0023	0.3311	
a_{13}	0.0001	0.0005	0.3158	0.7563	
a_{14}	-0.0010	0.0005	-2.1067	0.0513	
a_{15}	-0.0002	0.0042	-0.0545	0.9572	

The outcome of the ANOVA table for BOD suggests that Interaction model had a better prediction accuracy when the R-square values were compared.

The comparative analysis between the linear and interaction model predicted outcome was shown in figure 2.

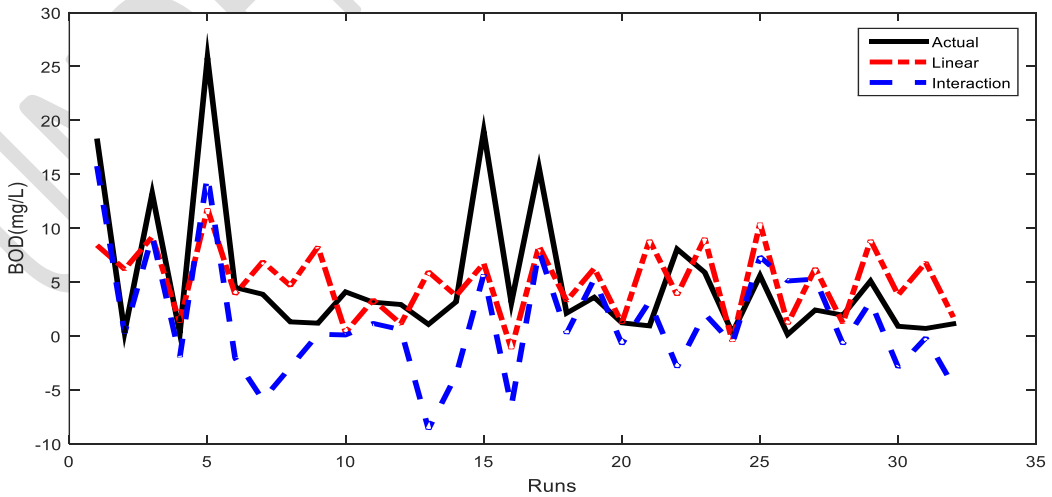

Figure 2; BOD RSM prediction comparative plot

From figure 2, it was seen that generally, the interaction RSM model predicted BOD had a better prediction than the linear model. This was affirmed by number of coincide points shown in figure 2 and affirmed by the statistical analysis performed.

The ANOVA table for COD linear and interaction models was shown in table 7 and table 8 respectively.

Table 7; Linear model

Coefficient variable	Coefficient values	Sum of square (SE)	T-statistics	P-value	Statistical parameters
a_0	339.6797	105.4300	3.2219	0.0034	R^2 = 0.2879
a_1	3.7392	2.1820	1.7136	0.0985	adjR^2 = 0.1510
a_2	-7.8563	14.3458	-0.5476	0.5886	mse = 592.7065
a_3	0.0006	0.0287	0.0221	0.9826	rmse = 24.3456
a_4	-0.5741	0.3094	-1.8555	0.0749	
a_5	-0.4680	0.3094	-1.5126	0.1424	

Table 8; interaction model

Coefficient variable	Coefficient values	Sum of square (SE)	T-statistics	P-value	Statistical parameters
a_0	532.6513	641.5447	0.8303	0.4186	R^2 = 0.3365
a_1	-18.9370	64.6581	-0.2929	0.7734	adjR^2 = 0.0117
a_2	-141.9645	446.6027	-0.3179	0.7547	mse = 897.4009
a_3	0.5839	0.8963	0.6514	0.5240	rmse = 29.9567
a_4	-1.3246	1.9269	-0.6874	0.5017	
a_5	-1.6891	8.1727	-0.2067	0.8389	
a_6	-3.1302	9.1067	-0.3437	0.7355	
a_7	-0.0077	0.0182	-0.4230	0.6779	
a_8	0.0872	0.1944	0.4485	0.6598	
a_9	-0.0415	0.1944	-0.2134	0.8337	
a_{10}	0.0076	0.1194	0.0639	0.9499	
a_{11}	0.5163	1.3264	0.3893	0.7022	
a_{12}	-0.5143	1.3264	-0.3877	0.7033	
a_{13}	-0.0016	0.0027	-0.6012	0.5561	
a_{14}	-0.0006	0.0027	-0.2082	0.8377	
a_{15}	0.0061	0.0245	0.2503	0.8056	

The outcome of the ANOVA table for COD suggests that Interaction model had a better prediction accuracy when the R-square values were compared.

The comparative analysis between the linear model predicted COD and the interaction model predicted COD was shown in figure 3.

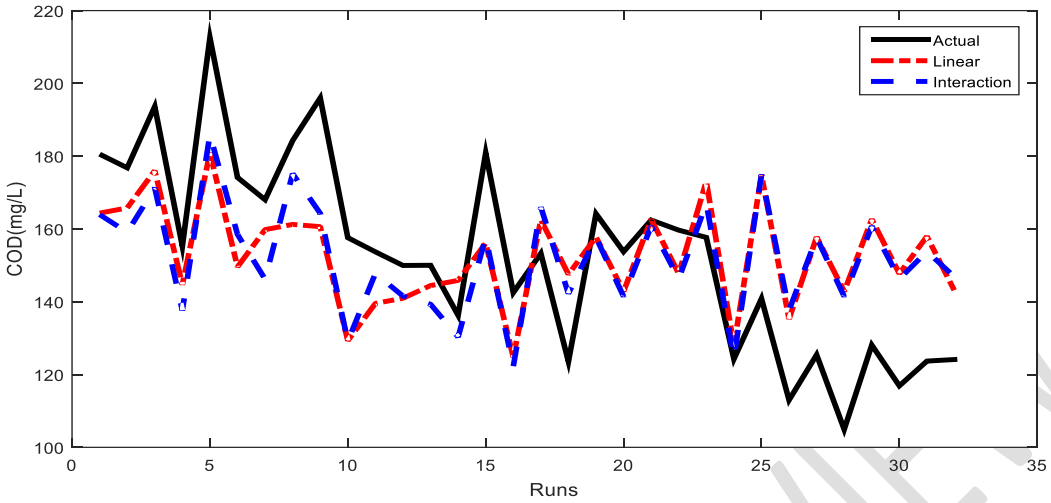

Figure 3; COD RSM prediction comparative plot

The outcome in figure 3 affirms that the interaction model predicted COD had a better prediction outcome than the linear model predicted COD in terms of tracking of the actual data. This was further affirmed by the statistical analysis performed.

The ANOVA table for Turbidity linear and interaction models were shown in table 9 and table 10 respectively.

Table 9; Linear model

Coefficient variable	Coefficient values	Sum of square (SE)	T-statistics	P-value	Statistical parameters
a_0	72.7069	73.0403	0.9954	0.3287	R^2 = 0.2530
a_1	-4.1383	1.5117	-2.7376	0.0110	adjR^2 = 0.1093
a_2	-4.0073	9.9385	-0.4032	0.6901	mse = 284.4702
a_3	0.0017	0.0199	0.0850	0.9329	rmse = 5.8147
a_4	0.0893	0.2144	0.4166	0.6804	
a_5	0.0939	0.2144	0.4380	0.6650	

Table 10; interaction model

Coefficient variable	Coefficient values	Sum of square (SE)	T-statistics	P-value	Statistical parameters
a_0	-104.2513	333.8372	-0.3123	0.7589	R^2 = 0.6073
a_1	-42.7905	33.6458	-1.2718	0.2216	adjR^2 = 0.2392
a_2	247.4808	232.3963	1.0649	0.3027	mse = 242.9947
a_3	0.5972	0.4664	1.2805	0.2186	rmse = 15.5883
a_4	0.8685	1.0027	0.8662	0.3992	
a_5	-1.8755	4.2528	-0.4410	0.6651	
a_6	2.4493	4.7388	0.5169	0.6123	

a_7	0.0032	0.0095	0.3421	0.7367	
a_8	0.1045	0.1012	1.0333	0.3168	
a_9	0.0235	0.1012	0.2322	0.8194	
a_{10}	0.0088	0.0621	0.1419	0.8889	
a_{11}	-0.9715	0.6902	-1.4074	0.1784	
a_{12}	1.5584	0.6902	2.2577	0.0383	
a_{13}	-0.0021	0.0014	-1.4982	0.1536	
a_{14}	0.0018	0.0014	1.2715	0.2217	
a_{15}	0.0008	0.0127	0.0642	0.9496	

The outcome of the ANOVA table for Turbidity suggests that Interaction model had a better prediction accuracy when the R-square values were compared.

The comparative plots of the linear and interaction models to the actual data was shown in figure 4.

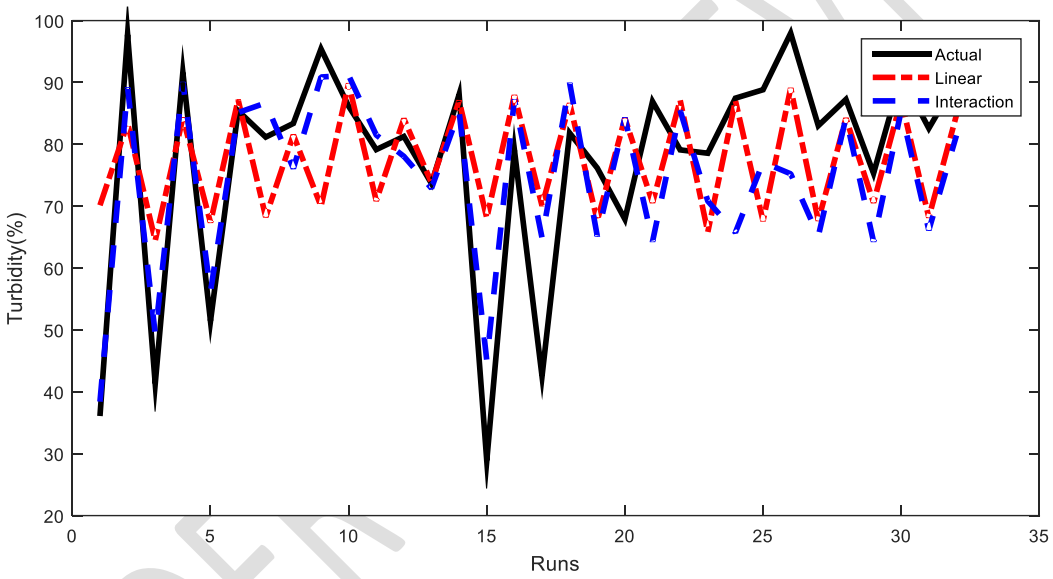

Figure 4; Turbidity RSM prediction comparative plot

The comparative plot in figure 4 affirms that interaction model had a better outcome as it had a better closeness to the actual data than that of the linear model predicted data. Hence, interaction model present a better optimal positions than the linear model.

The ANOVA table for colour linear and interaction models were shown in table 11 and table 12 respectively.

Table 11; Linear model

Coefficient variable	Coefficient values	Sum of square (SE)	T-statistics	P-value	Statistical parameters
a_0	76.7845	73.9548	1.0383	0.3087	R^2 = 0.2441
a_1	-4.1611	1.5306	-2.7186	0.0115	adjR^2 = 0.0987

a_2	-1.8438	10.0630	-0.1832	0.8560	mse = 291.6379
a_3	-0.0032	0.0201	-0.1567	0.8767	rmse = 17.0774
a_4	0.0621	0.2170	0.2862	0.7770	
a_5	0.0935	0.2170	0.4306	0.6703	

Table 12; interaction model

Coefficient variable	Coefficient values	Sum of square (SE)	T-statistics	P-value	Statistical parameters
a_0	-104.2513	333.8372	-0.3123	0.7589	R^2 = 0.5974
a_1	-42.7905	33.6458	-1.2718	0.2216	adjR^2 = 0.2200
a_2	247.4808	232.3963	1.0649	0.3027	mse = 252.4036
a_3	0.5972	0.4664	1.2805	0.2186	rmse = 15.8872
a_4	0.8685	1.0027	0.8662	0.3992	
a_5	-1.8755	4.2528	-0.4410	0.6651	
a_6	2.4493	4.7388	0.5169	0.6123	
a_7	0.0032	0.0095	0.3421	0.7367	
a_8	0.1045	0.1012	1.0333	0.3168	
a_9	0.0235	0.1012	0.2322	0.8194	
a_{10}	0.0088	0.0621	0.1419	0.8889	
a_{11}	-0.9715	0.6902	-1.4074	0.1784	
a_{12}	1.5584	0.6902	2.2577	0.0383	
a_{13}	-0.0021	0.0014	-1.4982	0.1536	
a_{14}	0.0018	0.0014	1.2715	0.2217	
a_{15}	0.0008	0.0127	0.0642	0.9496	

The outcome of the ANOVA table for Turbidity suggests that Interaction model had a better prediction accuracy when the R-square values were compared

The comparative plot of the linear and interaction model was shown in figure 5.

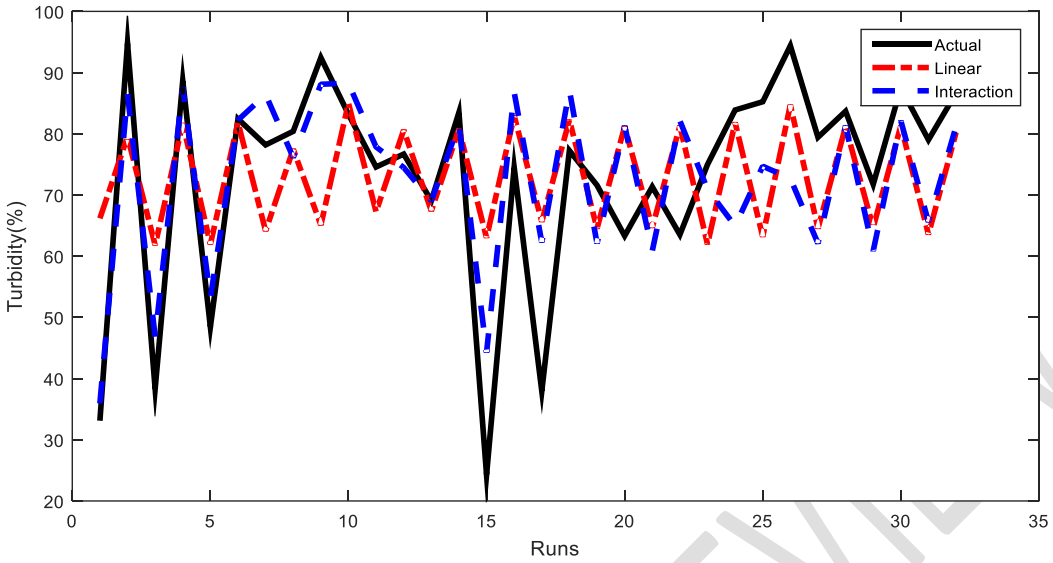

Figure 5; Colour RSM prediction comparative plot

Figure 5 affirms that the interaction model had a better prediction than the linear model and the prediction tracking deviation was lower in the interaction model data prediction than the linear model.

From the ANOVA table and the comparative plots presented, it was seen that interaction model had the best prediction accuracy and was used for the genetic algorithm optimization with the optimization iterations shown in table 13.

Table 13; Optimum conditions obtained with genetic algorithm

Responses and factors	Optimal conditions
BOD(mg/L)	4.33
COD(mg/L)	128.9
Turbidity (%)	39.87
Colour(%)	33.41
pH	5.5
Dosage(g)	0.68
Initial Conc (mg/L)	260
Temperature (K)	335
Time (mins)	50

The optimal response and the optimal conditions required to achieve the optimal repose executed in genetic algorithm was presented in table 13. At temperature of 335K, Initial concentration of 260mg/L, time of 50mins and dosage of 0.68g, the optimal responses of BOD 4.33mg/L, COD of 128.9mg/L, turbidity of 39.87% and colour of 33.41% were achieved.

Conclusion

This paper presented the purification process of Abattoir waste water using the synthesized nano-particles of crab shells. The experimental design was carried out with central composite design (CCD) based on pH, dosage, initial conc, temperature and time factors and the number of levels and number of experimental runs obtained were 5 and 50 respectively. The reponses considered were BOD, COD, turbidity and color. The outcome of the desing was taken to the laboratory to generate the values of the responses. The outcome of the experiment was subjected to the linear and interaction RSM models with ANOVA used to determine the performance of the models. It was found that interaction model had the best prediction performance and the outcome of the model was subjected genetic algorithm optimization. From the results obtained, it was found that at temperature of 335K, Initial concentration of 260mg/L, time of 50mins and dosage of 0.68g, the optimal responses of BOD 4.33mg/L, COD of 128.9mg/L, turbidity of 39.87% and colour of 33.41% were achieved.

For the suggestions for further studies, artificial intelligence models should be utilized in the prediction of the responses and should be compared with the outcome of the RSM models. Crab shell synthesized nano-particles should be utilized in the purification of other waste waters.

Reference

[1]Aniagor CO, Menkiti MC (2018) Kinetics and mechanistic description of adsorptiveuptake of crystal violet dye by lignifed elephant grass complexed isolate. J EnvironChem Eng. https://doi.org/10.1016/j.jece.2018.01.070

[2]Adeogun, O., Solarin, B. Ambrose, E. Ogunbadejo, H. Bolaji, D. Orimogunje, R. Ajulo, A. Olusola, A. Aroriode, R. Adeogun, M. (2011). Crab fishing and socio-economicconsiderations in lagos lagoon system in Nigeria, Int. J. Fish. Aquacult. 3, 118–125.

[3]Ali, A., Zafar, H., Zia, M., Haq, I., Phull, A. R., Ali, J. S., Hussain, A. (2016). Synthesis, characterization, applications, and challenges of iron oxide nanoparticles, Nanotechnology, Science and Applications. http://dx.doi.org/10.2147/NSA.S99986

[4]Braul, L., Viraraghavan, V., Corkal, D. (2001), Cold Water Effects on Enhanced Coagulation of High DOC, Low Turbidity Water, Water Qual. Res. J. Canada, 36 (4), 701–717

[5]Birima AH, Hammad HA, et al. (2013). Extraction of natural coagulant from peanut seeds for treatment of turbid water. IOP Conf Series Earth Environ Sci.,16:1–4.

[6]Elemile OO, Raphael DO, Omole DO, Oloruntoba EO, Ajayi EO, Ohwavborua NA (2019) Assessment of the impact of abattoir efuent on the quality of groundwater in a residential area of Omu-Aran, Nigeria. Environ Sci Eur 31:16. https://doi.org/10.1186/s12302-019-0201-5

[7]Ejımofor M. I. , Menkiti M. C. , Ezemagu I. G. (2020a). Comparative studies on removal of turbid-metric particles (TDSP) using animal based chito-protein and aluminium sulfate on paint wastewater (PWW). Sigma Journal of Engineering and Natural Sciences., 38(3): 1143-1159.

[8]Ejimofor, M.I., Ezemagu, G., Menkiti, M.C. (2020b). Biogas production using coagulation sludge obtained from paint wastewater decontamination: Characterization and anaerobic digestion kinetics, Current Research in Green and Sustainable Chemistry, 3, 100024. https://doi.org/10.1016/j.crgsc.2020.100024.

[9]Hatamie, A., Parham, H., Zargar, B., Heidari, Z., (2016). Evaluating magnetic nano-ferrofluid as a novel coagulant for surface water treatment, Journal of Molecular Liquids 219, 694–702. http://dx.doi.org/10.1016/j.molliq.2016.04.020

[10]Jeon C (2019) Removal of Cr (VI) from aqueous solution using amineimpregnated crab shells in the batch process. J Ind Eng Chem 77:111–117.

[11]Kundu, P. Debsarkar, A. Mukherjee, S. (2013). Treatment of slaughter house waste water in a sequencing batch reactor: performance evaluation and biodegradation kinetics, BioMed Res. Int. 11, 1–15.

[12] Kristianto, H., Reynaldi, E., Prasetyo, S., Sugih, A. (2020). Adsorbed leucaenaprotein on citrate modified Fe3O4 nanoparticles: synthesis, characterization, and its application as magnetic coagulant, Sustainable Environment Research, 30:32 https://doi.org/10.1186/s42834-020-00074-4.

[13]Okey-Onyesolu, C. F., Chukwuma, E. C., Okoye, C. C., & Onukwuli, O. D. (2020). Response Surface Methodology optimization of chito-protein synthesized from crab shell in treatment of abattoir wastewater. Heliyon, 6(10), e05186. https://doi.org/10.1016/j.heliyon.2020.e04468.

[14]Okuda T, Baes AU, et al. (1993). Improvement of extraction method of coagulation active components from moringa oleifera seed. Wat Res., 33(15):3373–3378.

[15]Okuda T, Baes AU, et al. (1999). Improvement of extraction method of coagulation active components from moringa oleifera seed. Wat Res. 1999;33(15):3373–3378.

[16]Okey-Onyesolu, C.F., Chukwuma E.C., Okoye C.C., Onukwuli O.D. (2020b). Response Surface Methodology optimization of chito-protein synthesized from crab shell in treatment of abattoir wastewater, Heliyon, e04468. https://doi.org/10.1016/j.heliyon.2020.e04468.

[17]Ogbeide OA (2015) Meat industry development in nigeria: implications of the consumers' perspective. Mayfair J Agribus Manag 1:59–75

[18]Ohale, P. E., Onu, C. E., Nwabanne, J. T., Aniagor, C. O., Okey-Onyesolu, C. F., Ohale, N. J. (2022). A comparative optimization and modeling of ammonia–nitrogen adsorption from abattoir wastewater using a novel iron-functionalized crab shell, Applied Water Science, 12:193. https://doi.org/10.1007/s13201-022-01713-4.

[19] Ohale, P. E., Onu, C. E., Ohale, N. J., Oba, S. N., (2020). Adsorptive kinetics, isotherm and thermodynamic analysis of fishpond effluent coagulation using chitin derived coagulant from waste Brachyura shell, Chemical Engineering Journal Advances, 4, 100036. https://doi.org/10.1016/j.ceja.2020.100036.

[20]Onu, C. E., Nwabanne, J. T., Ohale, P. E., Asadu. C. O. (2021). Comparative analysis of RSM, ANN and ANFIS and the mechanistic modeling in eriochrome black-T dye adsorption using modified clay, South African Journal of Chemical Engineering 36, 24 – 42. https://doi.org/10.1016/j.sajce.2020.12.003

[21]Panagopoulos, A. (2021). Energetic, economic and environmental assessment of zero liquid discharge (ZLD) brackish water and seawater desalination systems. Energy Conversion and Management, 235.

[22]Panagopoulos A (2022) Study and evaluation of the characteristics of saline wastewater (brine) produced by desalination and industrial plants. Environ Sci Pollut Res29:23736–23749. https://doi.org/10.1007/s11356-021-17694-x.

[23]Santos TRTd, Silva MF, et al. (2018). Magnetic coagulant based on moringa oleifera seeds extract and super paramagnetic nanoparticles: optimization of operational conditions and reuse evaluation. Desalin Water Treat., 106:226–237.

[24]Santos TRTd, Mateus GAP, et al. (2021). A simple and effective method for escherichia coli inactivation in aqueous medium using natural based superparamagnetic coagulant. Environ Prog Sustain Energy., 40(2): e13503.

[25] Soenen S. J, Himmelreich U, Nuytten N, Pisanic TR 2nd, Ferrari A, De Cuyper M. (2010). Intracellular nanoparticle coating stability determines nanoparticle diagnostics efficacy and cell functionality. Small., 6(19):2136–2145

[26] Tan, K., Hameed, B., (2017). Insight into the adsorption kinetics models for the removal of contaminants from aqueous solutions, J. Taiwan Inst. Chem. Eng. 74, 25–48.

[27] Von Sperling, M., Chernicharo, C. A., (2002). Urban wastewater treatment technologies and the implementation of discharge standards in developing countries, Urban Water 1, 105–114.

[28] Wang, N., Xu, Z., Xu, W., Xu, J., Chen, Y., Zhang, M., (2018). Comparison of coagulation and magnetic chitosan nanoparticle adsorption on the removals of organic compound and coexisting humic acid: A case study with salicylic acid, Chemical Engineering Journal 347, 514–524. https://doi.org/10.1016/j.cej.2018.04.131

[29] Wang, Y., Gu, X., Quan, J., et al. (2021). Application of magnetic fields to wastewater treatment and its mechanisms: A review. Science of the Total Environment 773, 145476. https://doi.org/10.1016/j.scitotenv.2021.145476.